JACS
JOURNAL OF THE AMERICAN CHEMICAL SOCIETY
Article
pubs.acs.org/JACS

Efficient Catalytic Interconversion between NADH and NAD$^+$ Accompanied by Generation and Consumption of Hydrogen with a Water-Soluble Iridium Complex at Ambient Pressure and Temperature

Yuta Maenaka,[†] Tomoyoshi Suenobu,[†] and Shunichi Fukuzumi*[,†,‡]

[†]Department of Material and Life Science, Graduate School of Engineering, Osaka University, ALCA, Japan Science and Technology Agency (JST), Suita, Osaka 565-0871, Japan

[‡]Department of Bioinspired Science, Ewha Womans University, Seoul 120-750, Korea

Supporting Information

ABSTRACT: Regioselective hydrogenation of the oxidized form of β-nicotinamide adenine dinucleotide (NAD$^+$) to the reduced form (NADH) with hydrogen (H_2) has successfully been achieved in the presence of a catalytic amount of a [C,N] cyclometalated organoiridium complex [Ir^{III}(Cp*)(4-(1*H*-pyrazol-1-yl-κN^2)benzoic acid-κC^3)-(H_2O)]$_2$ SO_4 [**1**]$_2$·SO_4 under an atmospheric pressure of H_2 at room temperature in weakly basic water. The structure of the corresponding benzoate complex Ir^{III}(Cp*)(4-(1*H*-pyrazol-1-yl-κN^2)-benzoate-κC^3)(H_2O) **2** has been revealed by X-ray single-crystal structure analysis. The corresponding iridium hydride complex formed under an atmospheric pressure of H_2 undergoes the 1,4-selective hydrogenation of NAD$^+$ to form 1,4-NADH. On the other hand, in weakly acidic water the complex **1** was found to catalyze the hydrogen evolution from NADH to produce NAD$^+$ without photoirradiation at room temperature. NAD$^+$ exhibited an inhibitory behavior in both catalytic hydrogenation of NAD$^+$ with H_2 and H_2 evolution from NADH due to the binding of NAD$^+$ to the catalyst. The overall catalytic mechanism of interconversion between NADH and NAD$^+$ accompanied by generation and consumption of H_2 was revealed on the basis of the kinetic analysis and detection of the catalytic intermediates.

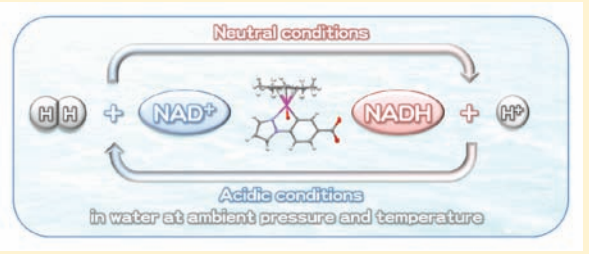

INTRODUCTION

In the natural photosynthesis of plants, electrons and protons taken from water using solar energy are used to reduce NAD(P)$^+$ by the action of ferredoxin-NADP reductase, generating the 1,4-dihydro form, i.e., NAD(P)H, which is used to reductively fix CO_2 as carbohydrates through the Calvin cycle.[1] On the other hand, in hydrogenase-containing photosynthetic organisms such as cyanobacteria and green algae, electrons taken from water using solar energy are used for the reduction of protons to hydrogen (H_2) rather than the reduction of NAD(P)$^+$ to NAD(P)H.[2−4] Both the oxidation of H_2 with NAD(P)$^+$ and the reduction of protons with NAD(P)H are catalyzed by hydrogenases.[2−4] Extensive efforts have so far been devoted to develop functional mimics of hydrogenase, which are able to reduce protons to H_2 or to oxidize H_2 to protons.[5−13] In the presence of appropriate enzymes, i.e., lactate dehydrogenase and horse liver dehydrogenase, regeneration of NADH from NAD$^+$ was made possible by using an organorhodium complex under pressurized H_2 (2.7 atm).[14] On the other hand, regeneration of NAD(P)H from NAD(P)$^+$ was catalyzed by Ru and Rh complexes under relatively high pressure of hydrogen (4.8 atm).[10] However, there has so far been no report on functional mimics of hydrogenase, which can catalyze the reversible interconversion between the oxidation of H_2 with NAD(P)$^+$ to produce protons and NAD(P)H and the reduction of protons with NAD(P)H to produce H_2 and NAD(P)$^+$.

Among various metal complexes, the half-sandwich iridium(III) complexes having pentamethylcyclopentadienyl (Cp*) ligand (IrCp*) are expected to be potential candidates for interconversion between NAD$^+$ and NADH (eq 1), because they have been used as catalysts for various types of transfer hydrogenation reactions and oxidative dehydrogenation reactions.[15−22] Under certain reaction conditions, the reactive intermediates in the catalytic cycle, e.g., a terminal hydride complex (Ir−H) or a dinuclear μ-hydride complexes (Ir−H−Ir) were stable even in water and isolable, and in some cases, their molecular structure can be defined by X-ray crystal structure analysis.[22a,b] Furthermore, molecular hydrogen (H_2) is activated by some IrCp*, and H_2 can be a reductant for the catalytic hydrogenation of imines,[23] dioxygen,[24] CO_2,[25−27] and other electrophilic substrates.[28−30] Especially, IrCp* in combination with a [C,N] cyclometalated ligand have recently been recognized to afford more efficient catalytic reactivity than that with α,α'-diamino or diimine ligands.[17a,19a,21a,23a]

$$NADH + H^+ \rightleftarrows NAD^+ + H_2 \quad (1)$$

Received: August 19, 2011
Published: November 28, 2011

   dx.doi.org/10.1021/ja207785f | J. Am. Chem.Soc. 2012, 134, 367−374

We report herein the first example of a functional mimic of hydrogenase using a water-soluble iridium aqua complex $[Ir^{III}(Cp^*)(4\text{-}(1H\text{-pyrazol-1-yl-}\kappa N^2)benzoic\ acid\text{-}\kappa C^3)(H_2O)]_2SO_4$, $[\mathbf{1}]_2\cdot SO_4$, having both Cp* and a [C,N] cyclometalated ligand, which can catalyze the oxidation of H_2 with NAD^+ to produce protons and NADH and also the reduction of protons with NADH to produce H_2 and NAD^+ under an atmospheric pressure at room temperature (eq 1). The direction of the reaction was found to be well controlled by pH.

EXPERIMENTAL SECTION

Materials. The following reagents were obtained with the best available purity and used without further purification unless otherwise noted: hydrogen hexachloroiridate, H_2IrCl_6 (4N grade, Furuya Metal Co., Ltd.), 1,2,3,4,5-pentamethylcyclopentadiene (>90%, Kanto Chemical Co., Inc.), 4-(1*H*-pyrazol-1-yl)benzoic acid (90% Aldrich Chemicals Co.), 3-(trimethylsilyl)propionic-2,2′,3,3′-d_4 acid sodium salt (>98%, Aldrich Chemicals Co.), β-nicotinamide adenine dinucleotide disodium salt hydrate, reduced form (Tokyo Chemical Industry Co., Ltd.), β-nicotinamide adenine dinucleotide, oxidized form (Oriental Yeast Co., Ltd.), acetonitrile (MeCN), boronic acid, potassium chloride, potassium carbonate, potassium formate, potassium dihydrogenphosphate, sodium borohydride, sodium hydroxide, diluted sulfuric acid (0.5 M) (Wako Pure Chemical Industries), disodium hydrogen phosphate (Aldrich Chemical Co.), sulfuric acid-d_2 in D_2O (95−97 wt % D_2SO_4, 99% D; Aldrich Chemical Co.), sodium hydroxide-*d* in D_2O (40 wt % NaOD, 99.5% D; Aldrich Chemical Co.), D_2O (99.9% D; Cambridge Isotope Laboratories), dimethylsulfoxide-d_6 (99.9% D; Cambridge Isotope Laboratories), H_2 (99.99%; Japan Air Gases Co.), D_2 (99.5%; Sumitomo Seika Chemicals Co., Ltd.), and standard gas (H_2 1.07%, CO_2 1.07%, CO 1.06%, N_2 96.8%; GL Sciences Co., Ltd.). $[Ir^{III}(Cp^*)(H_2O)_3]SO_4$ was synthesized according the reported procedure.[22a]

General Methods. All the experiments were carried out under an Ar or N_2 atmosphere by using standard Schlenk techniques unless otherwise noted. Purification of water (18.2 MΩ cm) was performed with a Milli-Q system (Millipore; Direct-Q 3 UV). ^1H and ^{13}C NMR spectra were recorded on JEOL JNM-AL300 spectrometer and Varian UNITY INOVA600 spectrometer. UV−vis absorption spectra were recorded on a Hewlett-Packard 8453 diode array spectrophotometer with a quartz cuvette (light-path length = 1 cm) at 298 K. Electrospray ionization mass spectrometry (ESI-MS) data were obtained by an API 150EX quadrupole mass spectrometer (PE-Sciex), equipped with an ion spray interface. The sprayer was held at a potential of +5.0 kV, and compressed N_2 was employed to assist liquid nebulization. The orifice potential was maintained at +30.0 V.

pH Adjustment. The pH values were determined by a pH meter (TOA, HM-20J) equipped with a pH combination electrode (TOA, GST-5725C). The pH of the solution was adjusted by using 1.00 M H_2SO_4/H_2O and 1.00−10.0 M $NaOH/H_2O$ without buffer unless otherwise noted. The pD of the solution was adjusted by using 95−97 wt % D_2SO_4 and 40 wt % NaOD without buffer unless otherwise noted. Values of pD were corrected by adding 0.4 to the observed values (pD = pH meter reading +0.4).[31]

X-ray Crystallographic Studies. Crystallographic data for $Ir^{III}(Cp^*)(4\text{-}(1H\text{-pyrazol-1-yl-}\kappa N^2)\text{-benzoate-}\kappa C^3)(H_2O)$ **2** has been deposited with the Cambridge Crystallographic Data Center as Supplementary Publication No. 814147. The data can be obtained free of charge from the Cambridge Crystallographic Data Center via www.ccdc.cam.ac.uk/data_request/cif. The intensity data sets were collected on Rigaku AFC-8 X-ray diffractometers with graphite monochromated Mo K_α radiation (λ = 0.71073 Å) using a ω scan technique. CrystalClear software was used for data reduction and empirical absorption corrections. The structures were solved by the direct methods using the Siemens SHELXTL version 5 package of crystallographic software. The difference Fourier maps based on these atomic positions yield the other non-hydrogen atoms. The hydrogen atom positions were generated theoretically, being allowed to ride on their respective parent atoms and included in the structure factor calculations with assigned isotropic thermal parameters. The structures were refined using a full-matrix least-squares refinement on F^2. All atoms except for hydrogen atoms were refined anisotropically. Crystal data for **2** are given in Table 1.

Table 1. X-ray Crystallographic Data for 2

	2
formula	$C_{20}H_{21}IrN_2O_3$
fw	529.62
crystal system	monoclinic
space group	$P2_1/n$
T, K	123
a, Å	11.533(3)
b, Å	10.250(3)
c, Å	15.157(4)
β, deg	102.2719(10)
V, Å^3	1750.9(8)
Z	4
no. of reflns	12694
no. of obsvd reflns	3948
parameters	236
$R1^a$	0.0362 ($I > 2.0\sigma(I)$)
$wR2^b$	0.0979 (all data)
GOF	1.076

$^aR1 = \Sigma\,||F_o| - |F_c||/\Sigma\,|F_o|$. $^bwR2 = [\Sigma\,(w(F_o^2 - F_c^2)^2)/\Sigma\,w(F_o^2)^2]^{1/2}$

Catalytic Hydrogenation of NAD^+ under an Atmospheric Pressure of H_2. Typically, a phosphate buffer (pH 6.0, 6.5, 7.0, and 8.0) or a borate buffer (pH 9.0 and 10.0) containing NAD^+ (0.77 mM), and $[\mathbf{1}]_2\cdot\mathbf{SO_4}$ (7.5 μM) was vigorously stirred under bubbling with H_2 (50 mL/min) at 298 K. The yield of NADH was determined by UV-absorption at λ = 340 nm. TOF values were determined on the basis of the progress of the reaction for initial 30 min. For measurements of the dependence of TOF on $[NAD^+]$, the concentration of NAD^+ was changed from 0.15 mM to 7.8 mM. For measurements of the dependence of the formation rate of NADH on [**2**], the concentration of **2** was changed from 6.8 μM to 30 μM.

Catalytic Hydrogenation of NAD^+ with HCOOK. Fifty microliters of a 5.0 M HCOOK aqueous solution was added to 2.0 mL of a phosphate buffer (pH 7.0) containing NAD^+ (0.77 mM) and $[\mathbf{1}]_2\cdot\mathbf{SO_4}$ (7.5 μM) at 298 K. The yield of NADH was determined by UV-absorption at λ = 340 nm. The TOF value was determined on the basis of the progress of the reaction for initial 15 min.

Catalytic Hydrogen Evolution from NADH. Typically, an aqueous NADH solution (0.10 mL, 6.6 μmol) was added to phthalate buffer (pH 4.1, 4.5, and 5.0) and phosphate buffer (pH 6.0 and 7.0) solutions (2 mL) containing $[\mathbf{1}]_2\cdot\mathbf{SO_4}$ (79 μg, 0.068 μmol) at 298 K. The amounts of evolved hydrogen were determined using a Shimadzu GC-14B gas chromatography (detector, TCD; column temperature, 50 °C; column, active carbon with the particle size 60−80 mesh; carrier gas, nitrogen gas). TOF values for the reaction at pH 4.1 and 4.2 were determined on the basis of the progress of the reaction for initial 10 min. TOF values for the reaction at pH 4.5 was determined on the basis of the progress of the reaction for initial 12 min. TOF values for the reaction at pHs 5.0, 6.0, and 7.0 were determined on the basis of the progress of the reaction for initial 20 min. No hydrogen evolution can be observed after 30 min in the absence of complex $[\mathbf{1}]_2\cdot\mathbf{SO_4}$. For measurements of the dependence of TOF on [NADH], the concentration of NADH was changed from 0.33 mM to 3.3 mM. For measurements of the dependence of hydrogen evolution rate on [**1**] and [**2**], the concentration of [**1**] and [**2**] was changed from 12 μM to 98 μM.

Catalytic Hydrogen Evolution from NADH in the Presence of NAD^+. An aqueous NADH solution (0.10 mL, 6.6 μmol) was added to a phthalate buffer (pH 4.5) solution (2.0 mL) containing

dx.doi.org/10.1021/ja207785f | J. Am. Chem.Soc. 2012, 134, 367−374

$[\mathbf{1}]_2\cdot SO_4$ (79 μg, 0.068 μmol) and NAD^+ (4.3 mg, 6.5 μmol) at 298 K. The evolved hydrogen was detected by GC until 30 min.

Determination of Rate-Determining Step in Hydrogenation of NAD^+ under an Atmospheric Pressure of H_2. A phosphate buffer solution (2.0 mL, pH 7.0) containing $[\mathbf{1}]_2\cdot SO_4$ (60 μM) was vigorously stirred for 9 min in a quartz cuvette (light-path length = 1 cm, head space = 3.3 mL) under an atmospheric pressure of hydrogen at 298 K. The total amount of hydrogen in the cuvette is the sum of the gas amount in the head space (~130 μmol) and that solubilized in water at pH 7.0 at 298 K (~1.6 μmol), which is 5.5×10^2 times larger than the amount of **2** (0.24 μmol). The amount of hydrogen in solution was estimated on the basis of Bunsen solubility coefficients for hydrogen in water.[32] Then, a phosphate buffer solution (50 μL, pH 7.0) containing NAD^+ (49 mM) was added to the solution. The progress of the reaction was monitored by the UV-absorption spectral change at λ = 340 nm.

UV–Vis Spectral Titration. Binding of NAD^+ to **2** was examined from the change in the absorbance of a phosphate buffer solution (pH 7.0) of **2** (2.0 mL, 0.13 mM) at λ = 330 nm by adding a phosphate buffer solution (5 μL to 110 μL, pH 7.0) of NAD^+ (9.6 mM) to the solution. The binding constant K was determined according to the procedure in our previous work (Figure S7 in SI).[33]

$[Ir^{III}(Cp^*)(4\text{-}(1H\text{-Pyrazol-1-yl-}\kappa N^2)\text{benzoic acid-}\kappa C^3)(H_2O)]_2SO_4$ ($[\mathbf{1}]_2\cdot SO_4$). An aqueous solution (50 mL) of $[Ir^{III}(Cp^*)(H_2O)_3](SO_4)$ (0.20 g, 0.423 mmol) and 4-(1*H*-pyrazol-1-yl)benzoic acid (0.085 g, 0.454 mmol) was stirred under reflux for 12 h, and then the solution was filtered with a membrane filter. The filtrate was evaporated under reduced pressure to yield a yellow powder of $[Ir^{III}(Cp^*)(4\text{-}(1H\text{-pyrazol-1-yl-}\kappa N^2)\text{benzoic acid-}\kappa C^3)(H_2O)]_2(SO_4)$, which was dried in vacuo {Yield: 94% based on $[Ir^{III}(Cp^*)(H_2O)_3](SO_4)$}. ^1H NMR (300 MHz, in DMSO-d_6, 298 K): δ (ppm) 1.75 (s, η^5-$C_5(CH_3)_5$, 15H), 6.99 (dd, J = 2.2 Hz, J = 2.7 Hz, 1H), 7.84 (dd, J = 8.4 Hz, J = 1.5 Hz, 1H), 7.91 (d, J = 8.4 Hz, 1H), 8.19 (d, J = 1.5 Hz, 1H), 8.33 (d, J = 2.2 Hz, 1H), 9.03 (d, J = 2.7 Hz, 1H). ^{13}C NMR (400 MHz, in DMSO-d_6, 298 K): δ (ppm) 168, 146, 144, 138, 135, 131, 130, 128, 111, 96.6, 9.06. Anal. Calcd for $Ir^{III}(Cp^*)(4\text{-}(1H\text{-pyrazol-1-yl-}\kappa N^2)\text{benzonate-}\kappa C^3)(H_2O)$: $C_{20}H_{23}O_3IrN_2$: C, 45.18%; H, 4.36%; N, 5.27%. Found: C, 44.90%; H, 4.30%; N, 5.11%. ESI-MS m/z 515 $[\mathbf{1} - H_2O]^+$.

RESULTS AND DISCUSSION

Synthesis, Structure, and pK_a Values of an Ir Aqua Complex. A water-soluble iridium aqua complex **1** was synthesized by the reaction of a triaqua complex $[Ir^{III}(Cp^*)(H_2O)_3]SO_4$ with 4-(1*H*-pyrazol-1-yl)benzoic acid in H_2O under reflux conditions. The aqua complex **1** can release protons from the carboxyl group and the aqua ligand to form the corresponding benzoate complex **2** and hydroxo complex **3**, respectively (Figure 1a). The pK_a values of complexes **1** and **2** were determined from the spectral titration to be pK_{a1} = 4.0 and pK_{a2} = 9.5, respectively (see Figure S1 in Supporting Information (SI)). The benzoate complex **2** is less soluble in water because of its neutral charge. The structure of **2** was successfully determined by X-ray single-crystal structure analysis. Figure 1b shows an ORTEP drawing of **2** which is a neutral-charged mononuclear Ir complex with no counterions.

Catalytic Hydrogenation of NAD^+. Hydrogenation of NAD^+ in the presence of a catalytic amount of **2** proceeds in slightly basic water at pD 8.0 as indicated by the ^1H NMR spectrum in Figure 2 (eq 2 and Scheme 1). It should be

$$NAD^+ + H_2 \rightarrow NADH + H^+ \quad (2)$$

emphasized that only the 1,4-isomer of NADH was exclusively produced by the reaction of NAD^+ with hydrogen in the presence of **2**.[34–36] The yield based on the amount of NAD^+ and turnover number (TON) reached up to 97% and 9.3 (90 min), respectively. To the best of our knowledge, this is the first example of 1,4-selective catalytic hydrogenation of NAD^+ to form NADH under an atmospheric pressure of H_2 with use of a metal complex (not an enzyme) as a catalyst in water at room temperature.

The progress of the reaction was monitored by the rise in the absorbance at λ = 340 nm due to NADH as shown by the time course of NADH concentration in Figure S2 in SI. From the slope of the linear dependence, the rate of formation of NADH was determined, increasing linearly with increasing the concentration of **2** at pH 7.0 as shown in Figure 3. In the

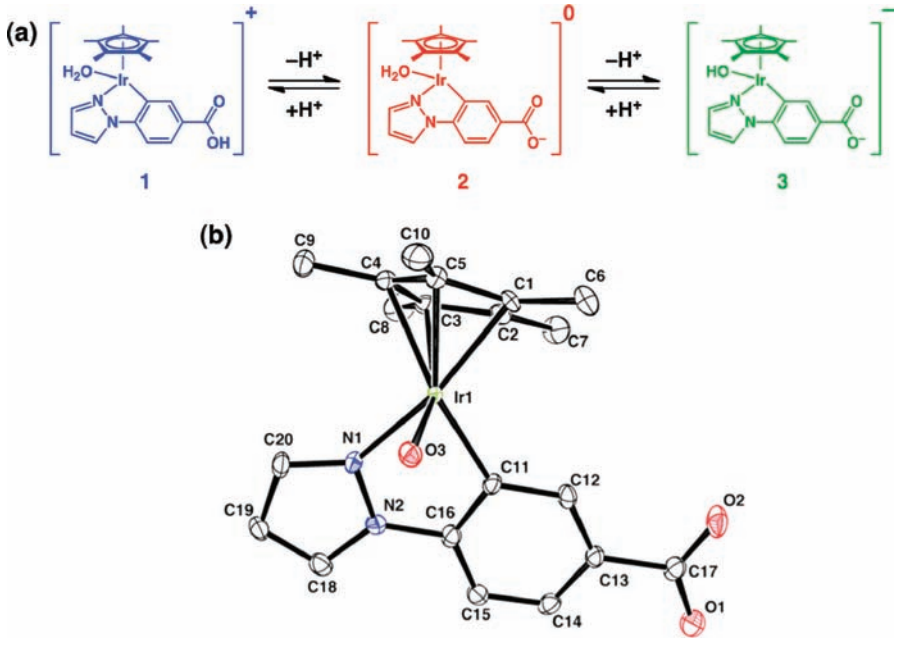

Figure 1. (a) Acid–base equilibria of iridium aqua complexes. (b) ORTEP drawing of **2**. Hydrogen atoms are omitted for clarity.

dx.doi.org/10.1021/ja207785f | J. Am. Chem.Soc. 2012, 134, 367–374

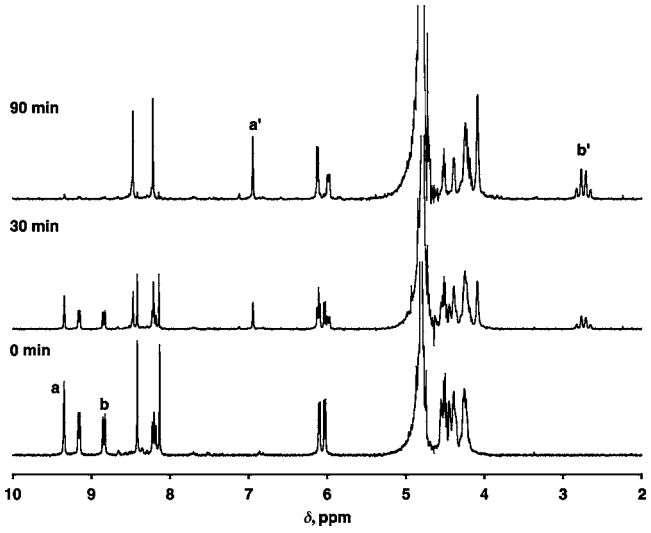

Figure 2. ^{1}H NMR spectral changes during the hydrogenation of NAD^+ (24 mM) with an atmospheric pressure of H_2 catalyzed by **2** (2.5 mM) in D_2O containing Na_2HPO_4 (130 mM) at 303 K at pD 8.0; a and a′ denote signals at 2 position of NAD^+ and NADH, respectively; b and b′ denote signals at 4 position of NAD^+ and NADH, respectively.[34]

absence of complex **2**, no reaction has occurred. The rate increased with increasing pH up to 6.5 and then decreased with further increase in pH as shown by the slope of the linear plots in Figure 4a. The decrease in the rate with further increase in pH from 6.5 results from the deprotonation of the aqua complex (Ir−H_2O: pK_a = 9.5) to afford the hydroxo complex (Ir−OH), which may not be active for the heterolysis of hydrogen. Complex **2** also promoted the reduction of NAD^+ to NADH in water at 298 K at pH 7.0 with $HCOO^-$ as a hydride donor[34,35,37] and the TOF value was determined from the change in UV absorption at λ = 340 nm to be 54 h^{-1} (Figure S3 in SI).

Catalytic Mechanism of Hydrogenation of NAD^+. Formation of the Ir−H complex under an atmospheric pressure of H_2 under slightly basic conditions was confirmed by ESI mass, ^{1}H NMR, and UV−vis absorption spectra (Figures S4 and S5 in SI). Thus, the Ir−H complex **5**, which was formed by the reaction of **2** with an atmospheric pressure of H_2, reduces NAD^+ to form 1,4-NADH selectively as shown in Scheme 2.

The rate-determining step in the catalytic hydrogenation of NAD^+ with H_2 is formation of the Ir−H complex, which reacts with NAD^+ rapidly to produce NADH, accompanied by regeneration of **2** as shown in Figure 5. The observed first-order rate constant (k_{obs}) of the formation of the Ir−H complex **5** under an atmospheric pressure of H_2 at pH 7.0 at 298 K was determined to be 6.3 × 10^{-2} s^{-1} from the first-order plot in Figure 5b. In contrast to the relatively slow formation of **5**, **5** immediately reacts with NAD^+ to produce NADH and **2**. Most of the hydride complex **5** (~70%) reacts with NAD^+ to produce **2** and NADH within 3 s as shown in right-hand part

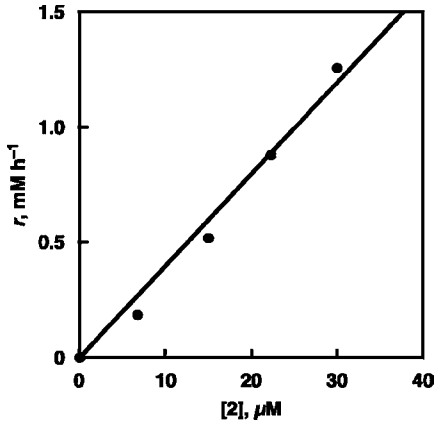

Figure 3. Plot of the formation rate (r, mM h^{-1}) of NADH vs the concentration of **2** in the catalytic hydrogenation of NAD^+ (0.77 mM) with H_2 to produce NADH under an atmospheric pressure of H_2 in the presence of **2** in deaerated phosphate buffer (pH 7.0) at 298 K. The formation rate (r) of NADH was determined on the basis of the progress of the reaction for initial 15 ([**2**] = 30 μM), 20 (22 μM), and 30 (15 μM and 6.8 μM) minutes, respectively.

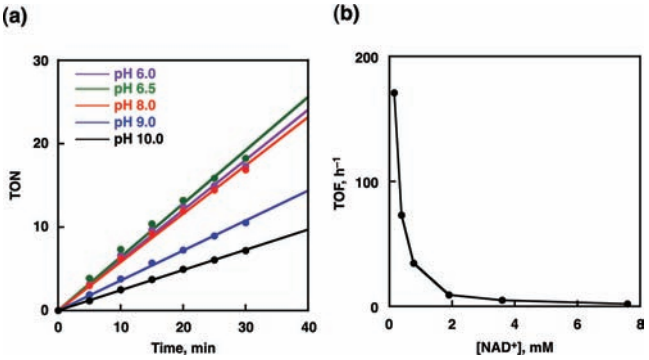

Figure 4. (a) Time course of the catalytic hydrogenation of NAD^+ (0.77 mM) with H_2 to form NADH in the presence **2** and **3** ([**2**] + [**3**] = 15 μM) in deaerated phosphate buffer (pH 6.0, 6.5, and 8.0) or borate buffer (pH 9.0 and 10.0) at 298 K at various pH values. Purple, green, red, blue, and black lines represent time profiles at pHs 6.0, 6.5, 8.0, 9.0, and 10.0, respectively. (b) Plot of TOF vs the concentration of NAD^+ in the catalytic hydrogenation of NAD^+ with H_2 to produce NADH under an atmospheric pressure in the presence of **2** ([**2**] = 15 μM) in deaerated phosphate buffer (pH 7.0) at 298 K. TOF values were determined on the basis of the progress of the reaction for initial 3 ([NAD^+] = 0.15 mM), 15 (0.39 mM), 30 (0.77 mM), and 120 (1.9 mM, 3.6 mM, and 7.8 mM) minutes, respectively.

in Figure 5a. This indicates that the formation of a hydride complex **5** is the rate-determining step in the overall catalytic cycle (Scheme 2).

It should be noted that TOF of the catalytic hydrogenation of NAD^+ decreased with increasing the concentration of NAD^+ (Figure 4b) due to the coordination of NAD^+ to **2** (Scheme 3), which makes it difficult to form the hydride complex via H_2

Scheme 1

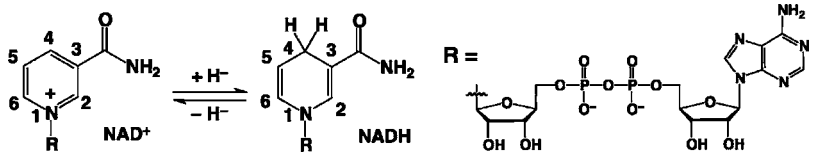

dx.doi.org/10.1021/ja207785f | J. Am. Chem.Soc. 2012, 134, 367−374

Scheme 2

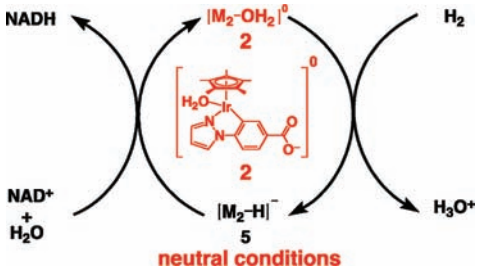

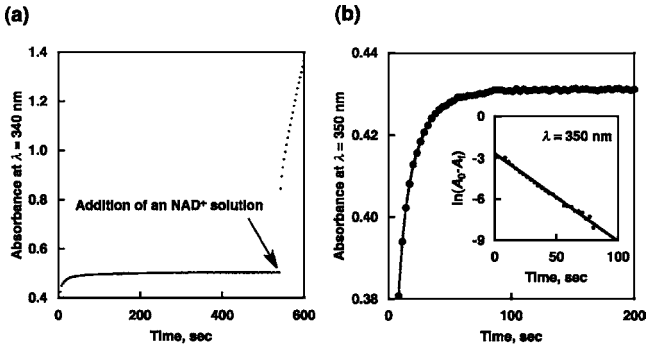

Figure 5. (a) Time course of absorbance at λ = 340 nm due to the formation of a hydride complex **5** in the reaction of **2** (0.12 mM) with an atmospheric pressure of hydrogen (left-hand part) and that due to the formation of NADH in the reaction of the hydride complex **5** with NAD^+ (1.2 mM) (right-hand part) in a phosphate buffer at 298 K (pH 7.0). The left-hand part in Figure 5a is magnified as shown in (b). (b) Time course of the absorbance at λ = 350 nm due to the formation of hydride complex **5** in the reaction of **2** (0.12 mM) with an atmospheric pressure of hydrogen in a phosphate buffer at 298 K (pH 7.0). Inset shows the first-order plots.

Scheme 3

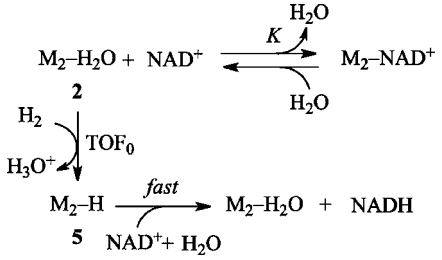

coordination (vide supra). In such a case, the formation rate of NADH (r_{NADH}, M s^{-1}) is given by eq 3, where $[\mathbf{2}]_i$ is the initial concentration of complex **2**. TOF_0 is the TOF value without the binding of NAD^+ to **2** and $TOF_0 = k_{obs}$. In eq 3, r is proportional to [**2**] as shown in Figure 3. The binding constant K (M^{-1}) is expressed by eq 4. When $[NAD^+] \gg [M_2\text{–}NAD^+]$ and $[NAD^+] \gg$ [NADH], TOF value is given by eq 5, which is converted to eq 6. As expected from eq 6, the plot of TOF^{-1} vs $[NAD^+]$ (Figure S6 in SI) shows a linear correlation. From the slope and intercept the binding constant (K) of NAD^+ with **2** is determined to be 1.4×10^4 M^{-1}, which agrees well with the value (1.6×10^4 M^{-1}) determined from the absorption changes due to the binding of NAD^+ with **2** (see Experimental Section, Figure S7 in SI, and the determination of the binding constant (K) in SI). In fact, the reaction of **2** with NAD^+ afforded a 1:1 complex as indicated by the ESI mass spectrum (Figure S8 in SI).

$$r_{NADH} = TOF_0[\mathbf{2}] = TOF[\mathbf{2}]_i = TOF([\mathbf{2}] + [M_2 - NAD^+]) \quad (3)$$

$$K = [M_2 - NAD^+]/[NAD^+][\mathbf{2}] \quad (4)$$

$$TOF = TOF_0[\mathbf{2}]/([\mathbf{2}] + [M_2 - NAD^+]) = TOF_0(1 + [M_2 - NAD^+]/[\mathbf{2}]) = TOF_0/(1 + K[NAD^+]) \quad (5)$$

$$1/TOF = 1/TOF_0 + K[NAD^+]/TOF_0 \quad (6)$$

Catalytic Hydrogen Evolution from NADH. In contrast to the catalytic hydrogenation of NAD^+ catalyzed by **2** under an atmospheric pressure of H_2 in a neutral aqueous solution, hydrogen was evolved from NADH in the presence of a catalytic amount of **1** in an acidic aqueous solution. The hydrogen evolution from NADH in water has so far been made possible under photoirradiation of an appropriate sensitizer at room temperature.[38,39] The oxidized product of NADH was confirmed to be NAD^+ by the ^1H NMR spectra (Figure S9 in SI). The yield and turnover number (TON) were determined to be 96% and 6.9 (20 min) by integrating the ^1H NMR signals of NAD^+ and NADH, respectively. Thus, the stoichiometry of the hydrogen evolution from NADH is given by eq 7.

$$NADH + H^+ \rightarrow NAD^+ + H_2 \quad (7)$$

Rates of the hydrogen evolution at various concentrations of **1** and **2** at pH 4.5 were determined from the time courses (Figure S10 in SI), increasing linearly with increasing concentrations of **1** and **2** as shown in Figure 6. On the other hand, the TOF values determined from the slope of linear plots of TON vs time (Figure 7a) increased linearly with the concentration of proton as shown in Figure 7b. The reaction of **1** and the deprotonated complex **2** with NADH

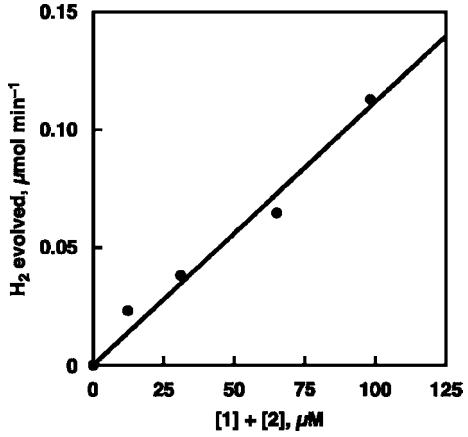

Figure 6. Plot of rates of the catalytic hydrogen evolution vs the concentration of **1** and **2** in the reaction of NADH (3.3 mM) with proton in the presence of **1** and **2** in deaerated phthalic buffer (2.0 mL) at 298 K at pH 4.5. TOF values were determined on the basis of the progress of the reaction for initial 6 min ([**1**] +[**2**] = 98 μM) and 12 min ([**1**] + [**2**] = 12 μM, 31 μM, and 65 μM).

dx.doi.org/10.1021/ja207785f | J. Am. Chem.Soc. 2012, 134, 367–374

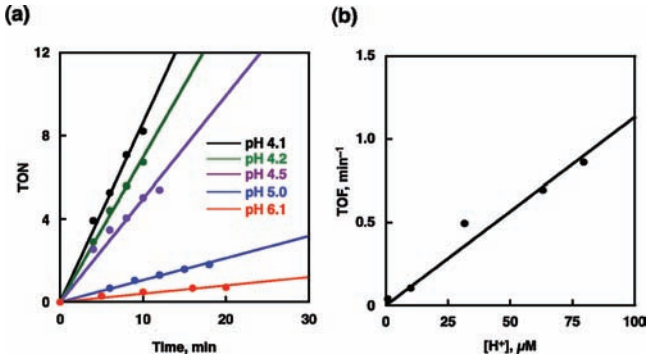

Figure 7. (a) Time course of hydrogen evolution in the reaction of NADH (3.3 mM) with proton in the presence of **1** and **2** ([**1**] + [**2**] = 65 μM) in deaerated phthalic buffer (pHs 4.1, 4.2, 4.5, and 5.0) or phosphate buffer (pH 6.1) solution (2.0 mL) at 298 K. Black, green, purple, blue, and red lines represent time profiles of hydrogen evolution at pHs 4.1, 4.2, 4.5, 5.0, and 6.1, respectively. (b) Plot of TOF for catalytic hydrogen evolution vs the concentration of H^+ in the reaction of NADH with proton in the presence of **1** and **2** ([**1**] + [**2**] = 65 μM) in deaerated phthalic buffer (pHs 4.1, 4.2, 4.5, and 5.0) or phosphate buffer (pH 6.1) solution (2.0 mL) at 298 K.

afforded the Ir-hydride complex as indicated by the ESI mass spectrum (Figure S11 in SI). The reaction of the hydride complex **4** with proton yields H_2, which is the rate-determining step in the catalytic cycle in Scheme 4 as indicated by the saturation behavior of TOF with the concentration of NADH (Figure 8).[40]

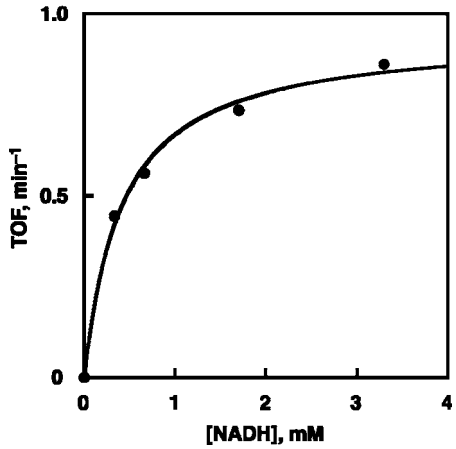

Figure 8. Plot of TOF for catalytic hydrogen evolution vs the concentration of NADH in the reaction of NADH with proton in the presence of **1** and **2** ([**1**] + [**2**] = 65 μM) in deaerated phthalic buffer (2.0 mL) at 298 K at pH 4.1. TOF values were determined on the basis of the progress of the reaction for initial 5 min ([NADH] = 0.33 mM, 0.66 mM, and 1.7 mM) and 10 min ([NADH] = 3.3 mM).

The catalytic cycle of hydrogen evolution from NADH with **1** is shown by Scheme 4, where catalyst **1** can be replaced by **2**. According to Scheme 4, the formation rate of H_2 (r_{H2}, M s^{-1}) is given by eq 8, where r_{H2} is proportional to the initial concentration of **1** and the concentration of proton as shown in Figures 6 and 7b, respectively. By applying the steady-state approximation to Scheme 4, [**4**] can be expressed by eq 9, where $[\mathbf{1}]_i$ is the initial concentrations of complex **1** ($[\mathbf{1}]_i$ = [**1**] + [**4**]). From eqs 8 and 9 is derived eq 10, where $K_M = (k_b[H_3O^+] + k_a^{-1})/k_a$. Equation 10 is converted to eq 11,

Scheme 4

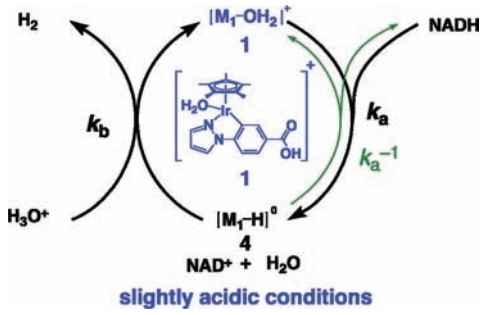

which predicts a linear correlation of TOF^{-1} vs $[NADH]^{-1}$. The linear plot of TOF^{-1} vs $[NADH]^{-1}$ is shown in Figure S12 in SI. From the slope and intercept of the linear plot, the k_b value is determined to be 1.9×10^2 M^{-1} s^{-1}, which is in good agreement with the k_b value (1.9×10^2 M^{-1} s^{-1}) determined independently from the slope of Figure 7b.

$$r_{H2} = k_b[\mathbf{4}][H_3O^+] = \mathrm{TOF}[\mathbf{1}]_i \quad (8)$$

$$k_a^{-1}[\mathbf{4}] + k_b[H_3O^+][\mathbf{4}] = k_a[\mathbf{1}][\mathrm{NADH}] = k_a([\mathbf{1}]_i - [\mathbf{4}])[\mathrm{NADH}] \quad (9)$$

$$\mathrm{TOF} = k_b[\mathrm{NADH}][H_3O^+]/(K_M + [\mathrm{NADH}]) \quad (10)$$

$$\mathrm{TOF}^{-1} = k_b^{-1}[H_3O^+]^{-1}K_M[\mathrm{NADH}]^{-1} + k_b^{-1}[H_3O^+]^{-1} \quad (11)$$

The hydrogen evolution is also retarded by the coordination of the product (NAD^+) to the Ir complexes **1** and **2**, which may prevent the formation of a hydride complex **4** (vide supra). Actually, no hydrogen was evolved in the presence of the same amount of NAD^+ as that of NADH in the reaction of NADH with proton in the presence of **1** (see Experimental Section).

Catalytic Interconversion between NADH and NAD^+. The pH dependence of TOF for both the hydrogen evolution from NADH and the formation of NADH from NAD^+ with **1** is summarized in Figure 9.[41] The black line in Figure 9, which shows an increase in TOF with a decrease in pH in the region between 4.1 and 7.0, well overlaps with the curve of the ratio of **1** (blue line in Figure 9), whereas the dashed line in Figure 9, which shows the TOF values for hydrogenation of NAD^+, well overlaps with the curve of the ratio of **2** (red line in Figure 9). This indicates that the complex **1** reacts with NADH to produce H_2 and the complex **2** reacts with H_2 to reduce NAD^+ to NADH. At pH 6.5, the TOF value for the formation of NADH is maximized (36 h^{-1}), whereas the TOF value for the hydrogen evolution reaches 52 h^{-1} at pH 4.1. Further decrease in pH resulted in decomposition of NADH due to acid-catalyzed hydration.[44] The change of the direction of the reaction in interconversion between NAD^+ and NADH depending on pH is largely consistent with the result of the thermodynamic analysis of the driving force (ΔG) of the reaction in eq 2 based on the redox potential of NADH/NAD^+ couple, $E^\circ = -0.32$ V vs NHE at pH 7.[45,46]

dx.doi.org/10.1021/ja207785f | J. Am. Chem.Soc. 2012, 134, 367–374

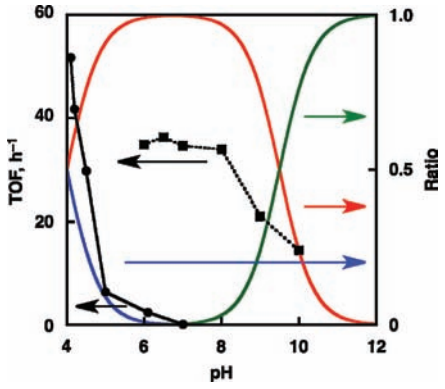

Figure 9. pH-dependence of the rate (TOF)[42] of H_2 evolution in the oxidation of NADH (3.3 mM) catalyzed by **1** and **2** ([**1**] + [**2**] = 0.18 mM) in deaerated H_2O at 298 K (●) and pH-dependence of the rate (TOF)[43] of formation of NADH in the reduction of NAD^+ (0.77 mM) by H_2 catalyzed by **2** and **3** ([**2**] + [**3**] = 15 μM) in deaerated H_2O at 298 K (■). Blue, red, and green solid lines correspond respectively to the amount of the ratios of complexes **1**, **2**, and **3** to the total amount of these complexes.

CONCLUSIONS

A water-soluble mononuclear [C,N] cyclometalated half-sandwich iridium complex, $[Ir^{III}(Cp^*)(4\text{-}(1H\text{-pyrazol-1-yl-}\kappa N^2)\text{-benzoic acid-}\kappa C^3)(H_2O)]_2(SO_4)$ $[\mathbf{1}]_2{\cdot}SO_2$ was newly synthesized and characterized by various spectroscopic methods and X-ray single-crystal structure analysis. **1** shows the deprotonation equilibrium (pK_{a1} = 4.0 and pK_{a2} = 9.5) to form an aqua complex **2** and the hydroxo complex **3** in water, depending on pH. Under an atmospheric pressure of H_2 at room temperature, NAD^+ was catalytically reduced by H_2 to produce 1,4-NADH selectively at a high yield (97% at pD 8.0) under the neutral and slightly basic conditions in the presence of a catalytic amount of an aqua complex **2**. At pH 6.5, the TOF for the formation of NADH reached up to 36 h^{-1}. Formation of a hydride complex **5** in the catalytic cycle was confirmed under slightly basic conditions in the absence of NAD^+ under an atmospheric pressure of H_2. At high NAD^+ concentrations, the hydrogenation reaction was retarded due to formation of a 1:1 complex between **2** and NAD^+. On the other hand, catalytic hydrogen evolution from NADH was made possible under slightly acidic conditions in the presence of a catalytic amount of an aqua complex **1** in a good yield (96% at pD 4.6). The TOF value of the hydrogen evolution reached up to 52 h^{-1} at pH 4.1. The saturation dependence of TOF on [NADH] is well explained by the formation of a hydride complex **4** followed by the rate-determining hydrogen evolution in the reaction of **4** with proton. Thus, **1** acts as an efficient catalyst and functional mimic of hydrogenase for interconversion between NADH and NAD^+, accompanied by generation and consumption of hydrogen at ambient pressure and temperature, depending on pH.

ASSOCIATED CONTENT

Supporting Information

Figures S1–S12, determination of the binding constant (K), derivation of ΔG. This material is available free of charge via the Internet at http://pubs.acs.org.

AUTHOR INFORMATION

Corresponding Author

fukuzumi@chem.eng.osaka-u.ac.jp

ACKNOWLEDGMENTS

This work was partially supported by a Grant-in-Aid (No. 20108010 to S.F. and No. 21550061 to T.S.) and a Global COE program, "the Global Education and Research Center for Bio-Environmental Chemistry" (to S.F.) from the MEXT, Japan, and NRF/MEST of Korea through WCU (R31-2008-000-10010-0) and GRL (2010-00353) Programs (to S.F.).

REFERENCES

(1) (a) Dau, H.; Haumann, M. *Coord. Chem. Rev.* **2008**, *252*, 273–295. (b) Yano, J.; Kern, J.; Sauer, K.; Latimer, M. J.; Pushkar, Y.; Biesiadka, J.; Loll, B.; Saenger, W.; Messinger, J.; Zouni, A.; Yachandra, V. K. *Science* **2006**, *314*, 821–825.

(2) (a) Magnuson, A.; Anderlund, M.; Johansson, O.; Lindblad, P.; Lomoth, R.; Polivka, T.; Ott, S.; Stensjö, K.; Styring, S.; Sundström, V.; Hammarström, L. *Acc. Chem. Res.* **2009**, *42*, 1899–1909. (b) Ghirardi, M. L.; Dubini, A.; Yu, J.; Maness, P. C. *Chem. Soc. Rev.* **2009**, *38*, 52–61.

(3) (a) Malki, S.; Saimmaime, I.; Luca, D. G.; Rousset, M.; Dermoun, Z.; Belaich., J. P. *J. Bacteriol.* **1995**, *177*, 2628–2636. (b) Soboh, B.; Linder, D.; Hedderich., R. *Microbiology* **2004**, *150*, 2451–2463. (c) Schut, G. J.; Adams, W. W. *J. Bacteriol.* **2009**, *191*, 4451–4457.

(4) Liebgott, P.-P.; De Lacey, A. L.; Burlat, B.; Cournac, L.; Richaud, P.; Brugna, M.; Fernandez, V. M.; Guigliarelli, B.; Rousset, M.; Léger, C.; Dementin, S. *J. Am. Chem. Soc.* **2011**, *133*, 986–997.

(5) (a) Ott, S.; Kritikos, M.; Åkermark, B.; Sun, L.; Lomoth, R. A *Angew. Chem., Int. Ed.* **2004**, *43*, 1006–1009. (b) Ott, S.; Kritikos, M.; Åkermark, B.; Sun, L. *Angew. Chem., Int. Ed.* **2003**, *42*, 3285–3288.

(6) (a) Ekström, J.; Abrahamsson, M.; Olson, C.; Bergquist, J.; Kaynak, F. B.; Eriksson, L.; Sun, L.; Becker, H.-C.; Åkermark, B.; Hammarström, L.; Ott, S. *Dalton Trans.* **2006**, 4599–4606. (b) Song, L.-C.; Tang, M.-Y.; Su, F.-H.; Hu, Q.-M. *Angew. Chem., Int. Ed.* **2006**, *45*, 1130–1133. (c) Na, Y.; Wang, M.; Pan, J.; Zhang, P.; Åkermark, B.; Sun, L. *Inorg. Chem.* **2008**, *47*, 2805–2810.

(7) (a) Ott, S.; Kritikos, M.; Åkermark, B.; Sun, L.; Lomoth, R. A. *Angew. Chem., Int. Ed.* **2004**, *43*, 1006–1009. (b) Schwartz, L.; Eriksson, L.; Lomoth, R.; Teixidor, F.; Viñas, C.; Ott, S. *Dalton Trans.* **2008**, 2379–2381.

(8) (a) Schwartz, L.; Eilers, G.; Eriksson, L.; Gogoll, A.; Lomoth, R.; Ott, S. *Chem. Commun.* **2006**, 520–522. (b) Eilers, G.; Schwartz, L.; Stein, M.; Zampella, G.; Gioia, L. D.; Ott, S.; Lomoth, R. *Chem.–Eur. J.* **2007**, *13*, 7075–7084.

(9) Ogo, S.; Kabe, R.; Uehara, K.; Kure, B.; Nishimura, T.; Menon, S. C.; Harada, R.; Fukuzumi, S.; Higuchi, Y.; Ohhara, T.; Tamada, T.; Kuroki, R. *Science* **2007**, *316*, 585–587.

(10) Wagenknecht, P. S.; Penney, J. M.; Hembre, R. T. *Organometallics* **2003**, *22*, 1180–1182.

(11) (a) Fukuzumi, S.; Kobayashi, T.; Suenobu, T. *J. Am. Chem. Soc.* **2010**, *132*, 1496–1497. (b) Fukuzumi, S.; Kobayashi, T.; Suenobu, T. *J. Am. Chem. Soc.* **2010**, *132*, 11866–11867.

(12) (a) Lee, C. H.; Dogutan, D. K.; Nocera, D. G. *J. Am. Chem. Soc.* **2011**, *133*, 8775–8777. (b) Matsubara, Y.; Koga, K.; Kobayashi, A.; Konno, H.; Sakamoto, K.; Morimoto, T.; Ishitani, O. *J. Am. Chem. Soc.* **2010**, *132*, 10547–10552. (c) Sato, S.; Arai, T.; Morikawa, T.; Uemura, K.; Suzuki, M. T.; Tanaka, H.; Kajino, T. *J. Am. Chem. Soc.* **2011**, *133*, 15240–15243.

(13) Bhaduri, S.; Mathur, P.; Payra, P.; Sharma, K. *J. Am. Chem. Soc.* **1998**, *120*, 12127–12128.

(14) Abril, O.; Whitesides, G. M. *J. Am. Chem. Soc.* **1982**, *104*, 1552–1544.

(15) (a) Suzuki, T. *Chem. Rev.* **2011**, *111*, 1825–1845. (b) Fujita, K.; Yamaguchi, R. *Synlett* **2005**, 560–571.

(16) (a) Page, M. I.; Stirling, M.; Blacker, J. *Tetrahedron Lett.* **2007**, *48*, 1247–1250. (b) Williams, J. M. J.; Saidi, O.; Blacker, A. J.; Farah, M. M.; Marsden, S. P. *Chem. Commun.* **2010**, *46*, 1541–1543. (c) Williams, J. M. J.; Saidi, O.; Blacker, A. J.; Farah, M. M.; Marsden, S. P. *Angew. Chem., Int. Ed.* **2009**, *48*, 7375–7378.

(17) (a) Ikariya, T.; Arita, S.; Koike, T.; Kayaki, Y. *Chem. Asian J.* **2008**, *3*, 1479−1485. (b) Ikariya, T.; Murata, K. *J. Org. Chem.* **1999**, *64*, 2186−2187. (c) Koike, T.; Ikariya, T. *Organometallics* **2005**, *24*, 724−730. (d) Ikariya, T.; Arita, S.; Koike, T.; Kayaki, Y. *Organometallics* **2008**, *27*, 2795−2802.
(18) (a) Andersen, R. A.; Golden, J. T.; Bergman, R. G. *J. Am. Chem. Soc.* **2001**, *123*, 5837−5838. (b) Skaddan, M. B.; Yung, C. M.; Bergman, R. G. *J. Am. Chem. Soc.* **2004**, *126*, 13033−13043. (c) Hostetler, M. J.; Butts, M. D.; Bergman, R. G. *J. Am. Chem. Soc.* **1993**, *115*, 2743−2752. (d) Bergman, R. G.; Alaimo, P. J.; Arndtsen, B. A. *Organometallics* **2000**, *19*, 2130−2143. (e) Ritter, J. C. M.; Bergman, R. G. *J. Am. Chem. Soc.* **1998**, *120*, 6826−6827.
(19) (a) Fujita, K.; Yoshida, T.; Imori, Y.; Yamaguchi, R. *Org. Lett.* **2011**, *13*, 2278−2281. (b) Fujita, K.; Tanino, N.; Yamaguchi, R. *Org. Lett.* **2007**, *9*, 109−111.
(20) (a) Yamamoto, N.; Obora, Y.; Ishii, Y. *Chem. Lett.* **2009**, *38*, 1106−1107. (b) Lofberg, C.; Grigg, R.; Whittaker, M. A.; Keep, A.; Derrick, A. *J. Org. Chem.* **2006**, *71*, 8023−8027.
(21) (a) Crabtree, R. H.; Zhou, M.; Schley, N. D. *J. Am. Chem. Soc.* **2010**, *132*, 12550−12551. (b) Soltani, O.; Ariger, M. A.; Vázquez-Villa, H.; Carreira, E. M. *Org. Lett.* **2010**, *12*, 2893−2895.
(22) (a) Ogo, S.; Makihara, N.; Watanabe, Y. *Organometallics* **1999**, *18*, 5470−5474. (b) Abura, T.; Ogo, S.; Watanabe, Y.; Fukuzumi, S. *J. Am. Chem. Soc.* **2003**, *125*, 4149−4154. (c) Himeda, Y.; Onozawa-Komatsuzaki, N.; Miyazawa, S.; Sugihara, H.; Hirose, T.; Kasuga, K. *Chem.—Eur. J.* **2008**, *14*, 11076−11081.
(23) (a) Xiao, J. L.; Wang, C.; Villa-Marcos, B. *Chem. Commun.* **2011**, *47*, 9773−9785. (b) Xiao, J. L.; Li, C. Q.; Wang, C.; Villa-Marcos, B. *J. Am. Chem. Soc.* **2008**, *130*, 14450−14451. (c) Ikariya, T.; Shirai, S.; Nara, H.; Kayaki, Y. *Organometallics* **2009**, *28*, 802−809.
(24) (a) Sicilia, E.; Chowdhury, S.; Himo, F.; Russo, N. *J. Am. Chem. Soc.* **2010**, *132*, 4178−4190. (b) Rauchfuss, T. B.; Heiden, Z. M. *J. Am. Chem. Soc.* **2007**, *129*, 14303−14310.
(25) Ogo, S.; Kabe, R.; Hayashi, H.; Harada, R.; Fukuzumi, S. *Dalton Trans.* **2006**, 4657−4663.
(26) (a) Himeda, Y. *Eur. J. Inorg. Chem.* **2007**, 3927−3941. (b) Himeda, Y.; Onozawa-Komatsuzaki, N.; Sugihara, H.; Kasuga, K. *Organometallics* **2007**, *26*, 702−712.
(27) Erlandsson, M.; Landaeta, V. R.; Gonsalvi, L.; Peruzzini, M.; Phillips, A. D.; Dyson, P. J.; Laurenczy, G. *Eur. J. Inorg. Chem.* **2008**, 620−627.
(28) Wu, X. F.; Corcoran, C.; Yang, S. J.; Xiao, J. L. *ChemSusChem* **2008**, *1*, 71−74.
(29) (a) Rauchfuss, T. B.; Letko, C. S.; Heiden, Z. M. *Eur. J. Inorg. Chem.* **2009**, 4927−4930. (b) Ohkuma, T.; Utsumi, N.; Watanabe, M.; Tsutsumi, K.; Arai, N.; Murata, K. *Org. Lett.* **2007**, *9*, 2565−2567.
(30) (a) Yamaguchi, R.; Ikeda, C.; Takahashi, Y.; Fujita, K. *J. Am. Chem. Soc.* **2009**, *131*, 8410−8412. (b) Wang, Z. X.; Li, H. X.; Jiang, J. L.; Lu, G.; Huang, F. *Organometallics* **2011**, *30*, 3131−3141.
(31) Glasoe, P. K.; Long, F. A. *J. Phys. Chem.* **1960**, *64*, 188−190.
(32) Crozier, T. E.; Yamamoto, S. *J. Chem. Eng. Data* **1974**, *19*, 242−244.
(33) Fukuzumi, S.; Kondo, Y.; Mochizuki, S.; Tanaka, T. *J. Chem. Soc., Perkin Trans.* **1989**, *2*, 1753.
(34) Yan, Y. K.; Melchart, M.; Habtemariam, A.; Peacock, A. F. A.; Sadler, P. J. *J. Biol. Inorg. Chem.* **2006**, *11*, 483−488.
(35) (a) Steckhan, E.; Herrmann, S.; Ruppert, R.; Dietz, E.; Frede, M.; Spika, E. *Organometallics* **1991**, *10*, 1568−1577. (b) Lo, H. C.; Leiva, C.; Buriez, O.; Kerr, J. B.; Olmstead, M. M.; Fish, R. H. *Inorg. Chem.* **2001**, *40*, 6705−6716. (c) Canivet, J.; Süss-Fink, G.; Štěpnička, P. *Eur. J. Inorg. Chem.* **2007**, 4736−4742.
(36) Selective formation of a 1,4-isomer of NADH has been achieved in the catalytic reduction of NAD^+ with HCOONa. See refs 34 and 35.
(37) (a) Ruppert, R.; Herrmann, S.; Steckhan, E. *J. Chem. Soc., Chem. Commun.* **1988**, 1150−1151. (b) Salmain, M.; Haquette, P.; Talbi, B.; Barilleau, L.; Madern, N.; Fosse, C. *Org. Biomol. Chem.* **2011**, *9*, 5720−5727.
(38) (a) Kotani, H.; Hanazaki, R.; Ohkubo, K.; Yamada, Y.; Fukuzumi, S. *Chem.−Eur. J.* **2011**, *17*, 2777−2785. (b) Fukuzumi, S.; Kotani, H.; Ono, T.; Ohkubo, K. *Phys. Chem. Chem. Phys.* **2007**, *9*, 1487−1492. (c) Yamada, Y.; Miyahigashi, T.; Kotani, H.; Ohkubo, K.; Fukuzumi, S. *J. Am. Chem. Soc.* **2011**, *133*, 16136−16145.
(39) (a) Amao, Y. *ChemCatChem* **2011**, *3*, 458−474. (b) Amao, Y.; Maki, Y.; Fuchino, Y. *J. Phys. Chem. C* **2009**, *113*, 16811−16815. (c) Okura, I.; Aono, S.; Kita, T. *Chem. Lett.* **1984**, 57−58.
(40) Because the iridium hydride complex **4** is a neutral-charged complex, the solubility of **4** in water is too low to be detected by ^1H NMR.
(41) The pK_a of the diphosphate moiety of both NAD^+ and NADH (~3.9) is lower than the pH range adopted in the measurements (pH > 4); see: Kishore, N.; Holden, M. J.; Tewari, Y. B.; Goldberg, R. N. *J. Chem. Thermodyn.* **1999**, *31*, 211−227.
(42) TOF values of the reactions at pHs 4.1 and 4.2 were determined from the progress of the reaction for initial 10 min. TOF values of the reactions at pH 4.5 were determined from the progress of the reaction for initial 12 min. TOF values for the reactions at pHs 5.0, 6.0, and 7.0 were determined from the progress of the reaction for the initial 20 min.
(43) TOF values were determined from the progress of the reaction for the initial 30 min.
(44) Johnson, S. L.; Tuazon, P. T. *Biochemistry* **1997**, *16*, 1175−1183.
(45) The driving force ($-\Delta G$) of hydrogenation reaction of NAD^+ with H_2 is calculated to be 15.3 kJ mol^{-1} at pH 6.5, which decreases significantly to 1.61 kJ mol^{-1} at pH 4.1. Thus, the direction of the reaction could be effectively controlled by changing pH. The ΔG values at various pH can be expressed by eq S8 in SI: $\Delta G = 21.8 - 5.71 \times$ pH (kJ mol^{-1}). The direction of the reaction could also be controlled by the pressure of H_2.
(46) Leduc, P.; Thevenot, D.; Buvet, R. *Bioelectrochem. Bioenerg.* **1976**, *3*, 491−508.